

# Green Chemistry

Accepted Manuscript



This is an *Accepted Manuscript*, which has been through the Royal Society of Chemistry peer review process and has been accepted for publication.

*Accepted Manuscripts* are published online shortly after acceptance, before technical editing, formatting and proof reading. Using this free service, authors can make their results available to the community, in citable form, before we publish the edited article. We will replace this *Accepted Manuscript* with the edited and formatted *Advance Article* as soon as it is available.

You can find more information about *Accepted Manuscripts* in the [Information for Authors](#).

Please note that technical editing may introduce minor changes to the text and/or graphics, which may alter content. The journal's standard [Terms & Conditions](#) and the [Ethical guidelines](#) still apply. In no event shall the Royal Society of Chemistry be held responsible for any errors or omissions in this *Accepted Manuscript* or any consequences arising from the use of any information it contains.



[www.rsc.org/greenchem](http://www.rsc.org/greenchem)



Journal Name

ARTICLE

## Selective reduction of nitroaromatics to azoxy compounds on supported Ag-Cu alloy nanoparticles through visible light irradiation

Received 00th January 20xx,  
Accepted 00th January 20xx

DOI: 10.1039/x0xx00000x

[www.rsc.org/](http://www.rsc.org/)

Zhe Liu, Yiming Huang, Qi Xiao\* and Huaiyong Zhu

The selective hydrogenation of aromatic nitrocompounds to their corresponding azoxy compounds is challenging in organic synthesis, which were typically performed under harsh reaction conditions. The core issue involved in this reduction is to finely control the product selectivity. Herein, we report an efficient photocatalytic process using supported silver-copper alloy nanoparticles (Ag-Cu alloy NPs) to selectively transform nitrobenzene to azoxybenzene by visible light irradiation under green mild reaction conditions. Ag-Cu alloy NPs can absorb visible light causing excited hot-electrons due to the localized surface plasmon resonance (LSPR) effect, and the excited electrons can activate the reactant molecule adsorbed on the NP surface to induce the reaction. The photocatalytic performance was affected by the ratio of Ag-Cu, and the catalyst with Ag-Cu molar ratio of 4-1 exhibited the optimal performance. Tuning the wavelength of incident light remarkably manipulate the product selectivity between azoxybenzene and aniline. Compared with pure Ag NPs, the alloying of Cu was found responsible for the product selectivity shifting from azobenzene to azoxybenzene. The reaction pathway was investigated to explain the selectivity difference and thus a tentative reaction pathway was proposed.

### Introduction

The selective reduction of nitroaromatics is one of the most significant reactions in organic synthesis,<sup>1-3</sup> because it produces important industrial intermediates such as amines,<sup>4</sup> azo and azoxy compounds.<sup>5</sup> Among them, azo and azoxy compounds attract particular interest for their widely application in the production of dyes, agrochemical, and pharmaceuticals.<sup>6-7</sup> Therefore, a variety of reduction processes have been developed to catalyse this reaction selectively to obtain the desired products.<sup>8-9</sup> Generally, the stoichiometric amount of reducing agents such as pressured hydrogen as well as transition metal catalysts are demanded, which may result in undesired by-products and the uncontrollability of product selectivity.<sup>10-11</sup> Grirrane *et al.* demonstrated that supported gold nanoparticle (Au NP) catalyst is capable of catalysing the reduction of nitro aromatics to the corresponding azo compounds through a two-step process.<sup>12</sup> However, high reaction temperature, pressured hydrogen and oxygen gas were required, the harsh reaction conditions not only increase the energy consumption but also the safety risk. From the point of view of green chemistry, it would be a promising process to drive the reduction under mild reaction conditions

through irradiation of visible light—the major component of abundant solar spectrum. In previous work, we have found that Au NPs supported on zirconium oxide (ZrO<sub>2</sub>) effectively catalyse the reductive coupling of nitrobenzene to azo compound under ambient pressure at 40°C by visible light irradiation,<sup>13</sup> this is mainly due to the reason that Au NPs can strongly absorb visible light through the localized surface plasmon resonance (LSPR) effect.<sup>14</sup> The LSPR effect is the collective oscillation of conduction electrons in the metal NPs induced by the electromagnetic field of the incident light.<sup>15</sup> Through this process, the light excited electrons of NPs can gain the energy from light and activate reactant molecules adsorbed on metal surface and trigger chemical reactions.<sup>16</sup> Apart from Au NPs, silver (Ag) and copper (Cu) NPs also exhibits strong light absorption in the visible range.<sup>17</sup> It has been reported that supported Ag NPs can be used as efficient photocatalyst under ultraviolet (UV) and visible light irradiation.<sup>18-19</sup> Very recently, Cu NPs supported on graphene were also been found to exhibit high photocatalytic activity for the reductive coupling of nitroaromatics to aromatic azo compounds under irradiation of solar spectrum.<sup>20</sup> However, the main products in both of the Au and Cu NPs catalysed reaction systems were azo compounds, and azoxy compounds appear as the intermediates during these processes which is not easily controllable. We thus envision the design of a high-performance catalyst for the selective reduction of nitro compounds to azoxy compounds under much milder and greener reaction conditions driven by visible light irradiation.

In the present study, we reported the selective reduction of nitroaromatics to azoxy compounds on Ag-Cu alloy NPs

School of Chemistry, Physics and Mechanical Engineering, Science and Engineering Faculty, Queensland University of Technology, Brisbane, QLD 4001, Australia.

E-mail: [q2.xiao@qut.edu.au](mailto:q2.xiao@qut.edu.au)

Fax: +61 7 3138 1804; Tel: +61 7 3138 1581.

† Electronic Supplementary Information (ESI) available: See DOI: 10.1039/x0xx00000x

under the irradiation of visible light. We successfully fabricated Ag-Cu alloy NPs with air stability by adjusting the Ag-Cu ratio. The Ag-Cu alloy NPs can efficiently drive the reduction of nitro aromatics and selectively yield azoxy compounds at moderate reaction temperature with the irradiation of visible light. From a green chemistry point of view, it would be a highly attractive and challenging goal to develop active, easily separable and reusable catalyst systems that can perform such desirable syntheses of aromatic azoxy compounds under more controlled, simplified, and greener conditions.

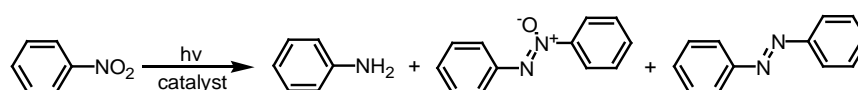
## Results and discussion

### Photocatalytic performance

Ag-Cu alloy NPs supported on  $ZrO_2$  ( $Ag-Cu@ZrO_2$ ) catalysts with different Ag:Cu ratio were prepared in the present study. The total metal amount (Ag+Cu) of the catalysts was maintained at 3 wt%. The photocatalytic reductions of nitrobenzene over Ag-Cu alloy NPs with different ratios under visible light irradiation were tested where isopropyl alcohol was acting as both the solvent and reducing agent. The reactions isolated from light while other reaction condition remained unchanged were carried out for comparison. The results are summarized in Table 1. Monometallic  $Ag@ZrO_2$  catalyst exhibited good catalytic activity with 90% conversion, while the control experiment in the dark only gave 25% conversion (entry 1). However, the main product was azobenzene (83%), and no azoxybenzene was detected.  $Cu@ZrO_2$  catalyst gave poor activity for this reaction with only 38% conversion under irradiation (entry 2), this is probably

due to the CuNPs cannot be stabilized on the  $ZrO_2$  surface, and the copper oxides on the surface strongly suppressed the catalytic activity. Interestingly, when using Ag-Cu alloy NPs as the catalyst, the main product selectivity was switched from azobenzene to azoxybenzene. The catalytic performance of alloy NPs was enhanced with higher Ag ratio, and the catalyst with Ag-Cu molar ratio of 4-1 exhibited the optimal performance (entry 3). Thus, the Ag-Cu (4-1) alloy  $@ZrO_2$  was selected as the optimal catalyst for the following experiments. Further increasing the amount of Ag or Cu may form large amount of metal oxide species on the surface which significantly suppressed the catalytic performance. The different Ag-Cu ratio did not affect the reaction selectivity. The general applicability of Ag-Cu (4-1) alloy  $@ZrO_2$  for the photocatalytic reduction of nitroaromatics with various functional groups was also investigated, the product selectivity can be maintained mainly at azoxy compounds and no azo product was detected (Table S1, ESI). These results confirmed that alloying Cu with Ag to form Ag-Cu alloy NPs can change the product selectivity for the reduction of nitroaromatic effectively at moderate conditions under visible light irradiation. Compared with some literature reported reaction conditions using Cu, Ag or Au catalysts for the reduction of nitrobenzene (Table 2), it can be seen that Ag-Cu alloy NPs can efficiently drive this reaction to obtain good azoxybenzene yield under mild conditions through visible light irradiation. Thus, to the best of our knowledge, this is the first example of selective reduction of nitro aromatics to yield azoxy compounds at moderate reaction temperature driven by "green" solar energy.

**Table 1.** Activity test and catalyst screening for reduction of nitrobenzene.

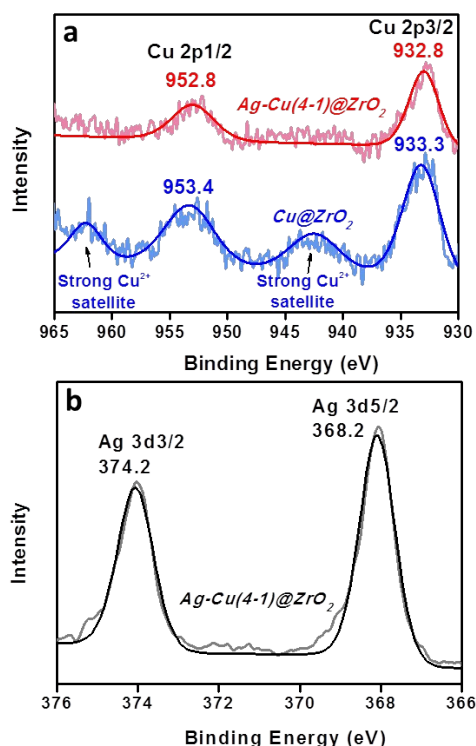


Entry	Ag:Cu <sup>[a]</sup>	Conv. (%) (dark)	Select. (%)			TON	TOF (h <sup>-1</sup> )
			Aniline	Azoxy	Azo		
1	Ag@ZrO <sub>2</sub>	90 (25)	17	0	83	32	2.0
2	Cu@ZrO <sub>2</sub>	38 (4)	12	76	12	8	0.5
3	4:1	96 (16)	14	86	0	32	2.0
4	1:1	74 (2)	18	82	0	21	1.3
5	1:4	57 (2)	16	83	1	14	0.9

Reaction condition: photocatalyst 50 mg, reactant 0.5 mmol, 3 mL isopropyl alcohol (IPA) as solvent, 0.15 mmol KOH as base, 1 atm argon atmosphere, reaction temperature 60°C, reaction time 16 h, and the light intensity was 0.8 W/cm<sup>2</sup>. The conversions and selectivity were analysed by gas chromatography (GC). [a] Molar ratio. TON=[amount of nitrobenzene (mol) × conversion]/[amount of Ag (mol)+amount of Cu (mol)], TOF=TON/reaction time (h).

**Table 2.** Comparison of the reaction conditions and achieved conversion of metal catalysts reported in literatures for the reduction of nitrobenzene.

Entry	Catalyst	Reaction conditions	Yield (%)		
			Aniline	Azobenzene	Azoxybenzene
1	Cu phthalocyanines <sup>21</sup>	70°C, 2h	93	-	-
2	Cu/HCOONH <sub>4</sub> <sup>22</sup>	120°C, 11h	86	-	-
3	Ag/TiO <sub>2</sub> <sup>18</sup>	1h	84	-	-
4	0.85 wt% Au/MgAl HT <sup>23</sup>	50°C, 3.5 h, 2 MPa H <sub>2</sub>	-	98	-
5	Au/ZrO <sub>2</sub> <sup>13</sup>	40°C, 5h, visible light	-	99	-
6	Cu/graphene <sup>20</sup>	90°C, 5h, visible light	-	96	-
7	5.0 % Pd/Al <sub>2</sub> O <sub>3</sub> <sup>24</sup>	65°C, 8h	-	-	44
8	Pd nanoparticle <sup>25</sup>	80°C, 24h	-	-	72
9	<b>Ag-Cu alloy@ZrO<sub>2</sub></b>	<b>60°C, 16h, visible light</b>	-	-	<b>75</b>

**Figure 1.** (a) XPS profile of Cu species in Ag-Cu (4-1)@ZrO<sub>2</sub> (red curve) and in Cu@ZrO<sub>2</sub> samples (blue curve). (b) XPS profile of Ag species in Ag-Cu (4-1)@ZrO<sub>2</sub> sample.

### Catalyst characterisation

Monometallic Cu NPs are unstable in the air, thus alloying Ag with Cu should be an effective approach to maintain its stabilization. To confirm the valence state of Cu species, the

sample was tested by X-ray photoelectron spectroscopy (XPS) and results are shown in Figure 1. For comparison, the monometallic Cu sample was also tested. It can be seen from Figure 1a that the XPS spectra of Cu in Ag-Cu (4-1)@ZrO<sub>2</sub> and Cu@ZrO<sub>2</sub> show much difference. First, two characteristic shake-up peaks at 942.7 eV and 962.2 eV can be observed in Cu@ZrO<sub>2</sub> sample (blue curve), which suggested that Cu(0) was oxidized to Cu(II) in the monometallic Cu sample. Thus, no further catalytic test was conducted with Cu@ZrO<sub>2</sub> sample due to it exists mainly as CuO. In the contrast, the shake-up peak disappeared in the Ag-Cu alloy sample (red curve), illustrating that Cu species existed in metallic state in alloy NPs when the Ag-Cu molar ratio was adjusted to 4-1.<sup>26</sup> On the other hand, as shown in Figure 1b, the binding energy peaks of Ag in alloy sample can be located at 368.2 eV and 374.2 eV attributed to the zero valence of Ag, thus the metallic state of Ag in bimetallic alloy can be confirmed.<sup>27</sup> These results suggested that we may use alloying effect to maintain the metal nanoparticles' stability.

The representative transmission electron microscopy (TEM) images of the catalyst are shown in Figure 2. The Ag-Cu alloy NPs are well distributed on the ZrO<sub>2</sub> crystal surface (Figure 2a) with a mean particle size of 7 nm (Figure 2b). The high resolution (HR)-TEM image indicates that the crystal face of alloy nanoparticle is predominantly (111) face and the space of lattice fringe is 0.23 nm (Figure 2c). Figure 2d is a cross-sectional compositional line profile analysis of the energy dispersion X-ray (EDX) spectrum from TEM for a typical Ag-Cu (4-1) alloy NP, showing that the NP consists of both Ag and Cu elements distributed uniformly, which suggests that the two metals exist as binary alloy NPs in this sample. The composition of Ag and Cu elements in the alloy catalysts was also analysed from the EDX spectrum (Figure 2e). The Ag/Cu

ratio (4/1) is well matched with the initial experimental design. This was further supported by the detailed data summarized from both TEM and scanning electron microscopy (SEM) analysis (Table S1, Figure S1 and S2, ESI). The appearance of both metals, Ag and Cu, in the elemental mapping from TEM also confirmed the alloy character of the bimetallic Ag-Cu catalyst (Figure 2f).

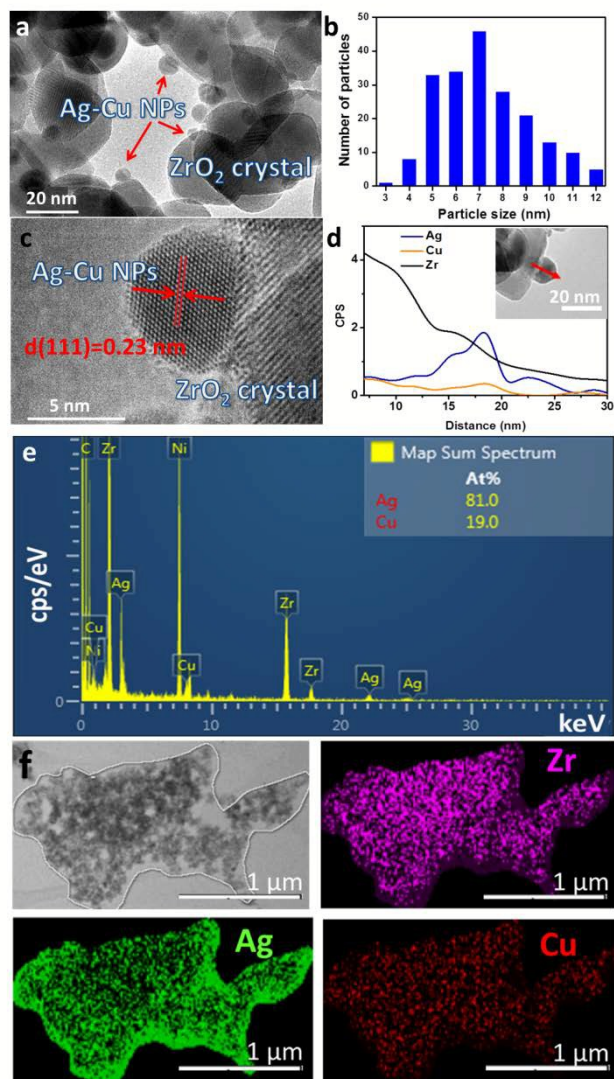


**Figure 2.** (a) TEM image of Ag-Cu (4-1)@ZrO<sub>2</sub> sample. (b) Particle size distribution of Ag-Cu (4-1)@ZrO<sub>2</sub> sample. (c) HR-TEM image of an Ag-Cu (4-1)@ZrO<sub>2</sub> particle. (d) The line profile analysis of Ag-Cu NP corresponding to the particle indicated by the red arrow in inset. (e) EDX spectrum of Ag-Cu (4-1)@ZrO<sub>2</sub> samples. (f) EDX mapping of Zr, Ag and Cu elements.

One of the important features of the photocatalyst is its light absorption property, which represents the light absorption ability of the catalyst. The diffuse reflectance UV-visible (DR-UV-vis) spectra of supported Ag-Cu alloy NPs are shown in Figure 3. The light absorption peak of the Ag-Cu (4-1) NPs is located at 408 nm while the light absorption peak of pure Ag NPs is 392 nm which is attributed to the LSPR effect.

The ZrO<sub>2</sub> support exhibits negligible absorption of light with wavelengths above 400 nm, thus the support itself does not show any light absorption in the visible range.<sup>28</sup> As a result, the absorption of the photocatalyst in the visible light range is due to the formation of Ag-Cu alloy NPs, indicating that the alloy NPs may have the potential to utilise the irradiation energy delivered by the wider range of solar spectrum.

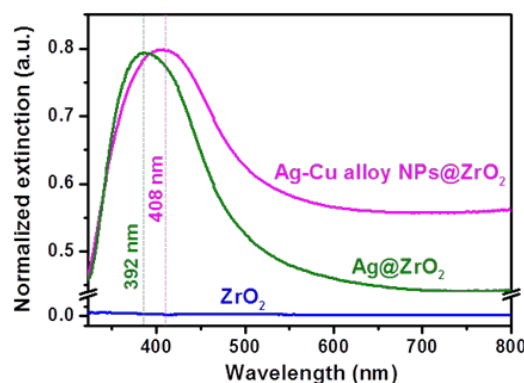


**Figure 3.** The normalized DR-UV-vis spectra of the Ag-Cu (4-1)@ZrO<sub>2</sub> catalyst, as well as its comparison with monometallic Ag@ZrO<sub>2</sub> and ZrO<sub>2</sub> support.

The X-ray diffraction (XRD) patterns of the Ag@ZrO<sub>2</sub> and Ag-Cu alloy@ZrO<sub>2</sub> photocatalysts are shown in Figure 4. It can be seen that the diffraction peaks of all the samples can be indexed to a monoclinic structure of the ZrO<sub>2</sub> crystal.<sup>29</sup> The reflection peaks of Ag and alloy cannot be identified due to the low metal content (3 wt%). As a result, the loading of alloy NP have no impact on the crystal structure of ZrO<sub>2</sub> supporting material.

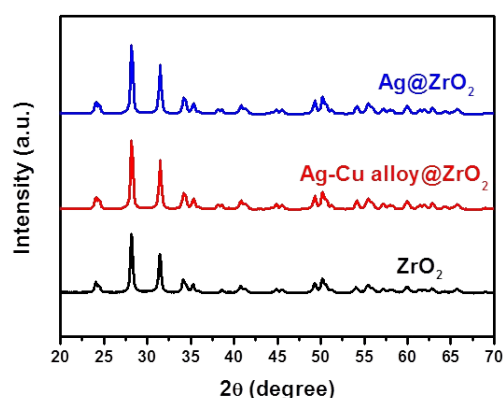


**Figure 4.** The XRD patterns of the photocatalysts.

#### Impact of wavelength and light intensity

To further understand the contribution of light and verify the photocatalytic mechanism, the dependence of catalytic activity on wavelength and light irradiance (intensity) was investigated. Action spectrum presents the mapping of the wavelength dependent photocatalytic rate and the light extinction spectrum, which is a useful way to determine which wavelength

of light can drive reaction effectively.<sup>30-31</sup> We conducted the reduction of nitrobenzene over Ag-Cu (4-1) alloy photocatalyst as model reaction. Five LED lamps with wavelengths of  $400 \pm 5$ ,  $470 \pm 5$ ,  $530 \pm 5$ ,  $590 \pm 5$ , and  $620 \pm 5$  nm were used as light source. The reaction rates were calculated and presented in apparent quantum yield (AQY).<sup>32-33</sup> The AQY for the reduction of nitrobenzene were compared with the light absorption spectrum of Ag-Cu alloy NPs. It can be seen from Figure 5 that the trend of AQY well matches with the light absorption curve of the Ag-Cu alloy photocatalyst. The most significant enhancement of reaction rate was observed at 400 nm, where LSPR peak of Ag-Cu alloy NPs located. The action spectrum suggested that the enhancement of the catalytic performance was mainly due to the light absorption of the alloy NPs. The metal electrons gain sufficient energy from the LSPR effect under irradiation which can be then transferred into the reactant molecules absorbed on the metal surface to induce the reaction. Here, we can confirm that it is the alloy NPs that act as an antenna that harvest visible light enhancing the catalytic reaction activity.

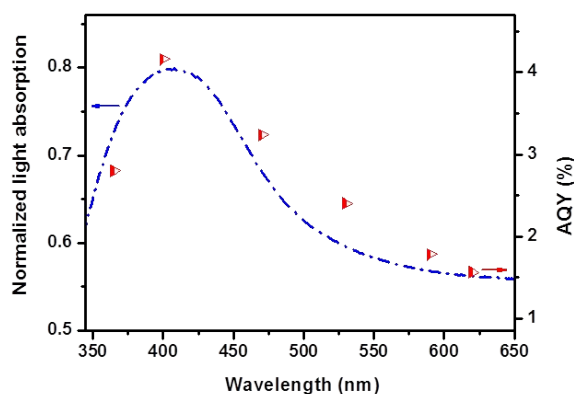


**Figure 5.** Photocatalytic action spectrum for the reduction of nitrobenzene using Ag-Cu(4-1)@ZrO<sub>2</sub> photocatalyst. The light absorption spectrum (left axis) is the DR-UV/vis spectrum of the supported Ag-Cu(4-1)@ZrO<sub>2</sub> catalyst.

**Table 3.** Performance of Ag-Cu (4-1)@ZrO<sub>2</sub> photocatalyst in nitrobenzene reduction with irradiation of different wavelengths.

Wavelength (nm)	AQY (%)	Conv. (%)	Select. (%)	
			Aniline	Azoxy
365	2.8	35	90	0
400	4.2	60	34	58
470	3.2	55	25	75
530	2.4	46	19	81
590	1.8	38	16	84
620	1.6	35	11	89

Reaction condition: photocatalyst 50 mg, reactant 0.5 mmol, 3 mL IPA as solvent, 0.15 mmol KOH as base, 1 atm argon atmosphere, reaction temperature 70°C, reaction time 16 h, and the light intensity was 0.2 W/cm<sup>2</sup>. The conversions and selectivity were analysed by GC.

In addition to the reaction rate, we also found that the light wavelength can remarkably affect the product selectivity as shown in Table 3. When shining by the light with the shortest wavelength (365 nm), the highest selectivity to aniline was obtained and the selectivity decreased with the increasing of wavelength. Such result illustrated that we can manipulate the selectivity of nitrobenzene reduction by the wavelength of incident light. The possible reason is that transfer of the energetic electrons to transform nitrobenzene to aniline require greater energy than that of azoxybenzene, light with shorter wavelengths can excite electron of metal to higher energy level and have greater chance to overcome the energy barrier to yield aniline.

Besides wavelength dependence, the impact of light intensity is another important feature of the photocatalytic reactions.<sup>34</sup> The dependence of catalytic activity on light irradiation intensity was investigated and the results is shown in Figure 6. The conversion in the dark was regarded as the contribution of thermal effect, we conducted the reaction under different irradiance (from 0.5 to 1.0 W/cm<sup>2</sup>) while all the other reaction conditions were kept identical. We can see that the conversion increased with the increasing of light irradiance. The contributions of irradiation to the conversion efficiency were calculated by subtracting the extent of conversion achieved in the dark from the overall extent of the irradiated system.<sup>35</sup> To be more clear, the contribution of irradiation accounts for only 66% for the reaction when the irradiation was 0.5 W/cm<sup>2</sup>, while it increased to 83% with the irradiation of 1.0 W/cm<sup>2</sup>. It shows that the contribution of irradiation effect is increasing with the raise of light intensities, this is due to the reason that with higher light intensity, larger amount of light energetic electrons can be excited thus give higher reaction rate.

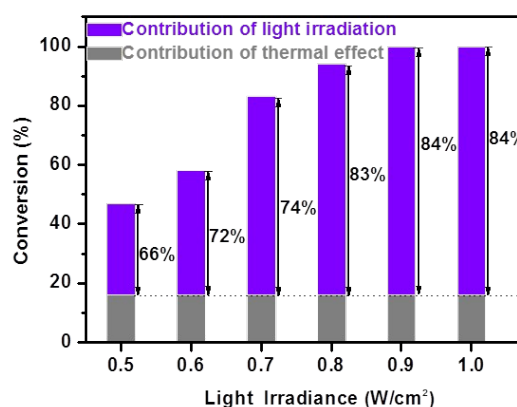


**Figure 6.** Dependence of the catalytic activity of Ag-Cu (4-1)@ZrO<sub>2</sub> for reduction of nitrobenzene on the intensity of light irradiation. The numbers with percentages show the contribution of the light irradiation effect. A photometer was used to measure the light intensity; the other experimental conditions were kept the same.

The relationship of reaction activity with the light irradiance and wavelength confirmed that the light excited

energetic electrons play the key role in photocatalysed reactions. The population of energetic electrons can be enhanced by applying higher light irradiance and turning the wavelength of irradiation.

### Impact of temperature

Another important feature of the photocatalytic process on metal NP catalysts is that the photocatalytic activity of the NPs can be increased by elevating the reaction temperature.<sup>36-37</sup> As shown in Figure 7, higher reaction yield was achieved with the temperature raising both under irradiation and in the dark. However, the contribution of light irradiation reduced with the rising of reaction temperature. For example, when at 50°C, the difference between the light reaction and dark reaction was 68% accounting for 97% of the total conversion, which decreased to 61% when the temperature was increased to 70°C. Under thermal heating conditions, the thermal activated electrons of metal NPs can activate adsorbed molecules and trigger the chemical reactions as well. At high reaction temperature, larger population of thermal activated electrons were generated with greater chance to surmount the activation barrier, thus it is easier for the activation of the reactions. Meanwhile, the vibrational states of the adsorbed molecules were excited by high reaction temperature and therefore the activation of substrate molecules is much easier.<sup>35</sup> This theory can also explain that the contribution decreases as the reaction temperature was raised. At low temperature, the thermal energy is insufficient to activate metal electrons to overcome the activation barrier therefore light excited electrons dominates the catalytic activity. In contrast, high reaction temperature can generate a remarkable amount of excited metal electrons capable of crossing activation barrier thus the contribution of light energy is suppressed.

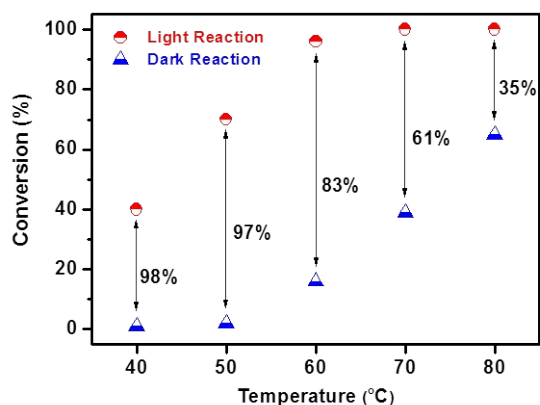


**Figure 7.** Dependence of catalytic activity on different reaction temperatures for reduction of nitrobenzene under a thermal heating process in dark (blue triangles) and the light irradiation process (red circles). The light intensity was  $0.8 \text{ W/cm}^2$ .

The effect of temperature on the product selectivity was also investigated. As shown in Table 4, with the raising of

temperature, we did not obtain any significant changing of product selectivity. It can be concluded that temperature has limited influence on selectivity of nitrobenzene reduction compared with that of light wavelength in this reaction.

**Table 4.** Performance of Ag-Cu (4-1)@ZrO<sub>2</sub> photocatalyst in nitrobenzene reduction at different temperatures.

Temp (°C)	Conv. (%)	Select. (%)	
		Aniline	Azoxy
40	40	27	73
50	70	21	78
60	96	14	86
70	100	11	85
80	100	13	87

Reaction condition: photocatalyst 50 mg, reactant 0.5 mmol, 3 mL isopropyl alcohol (IPA) as solvent, 0.15 mmol KOH as base, 1 atm argon atmosphere, reaction time 16 h, and the light intensity was  $0.8 \text{ W/cm}^2$ . The conversions and selectivity were analysed by GC.

Additionally, the apparent activation energy of the reaction can be calculated by the reaction rate at different temperatures using Arrhenius equation. We conducted the reduction of nitrobenzene at different temperatures: 30°C, 40°C, 50°C, 60°C, 70°C and 80°C both under irradiation and in the dark (thermal process). The apparent activation energy of light reaction and dark reaction are shown in Figure 8, it can be seen that the apparent activation energy for reduction of nitrobenzene in the dark is  $104.4 \text{ kJ mol}^{-1}$  while only  $20.4 \text{ kJ mol}^{-1}$  for the reaction under irradiation. The visible light irradiation reduced the activation energy of the reaction by  $80 \text{ kJ mol}^{-1}$ , which accounts for 80.4% of the apparent activation energy in the thermal reaction. The reduced apparent activation energy in irradiation indicates the contribution of light irradiation.<sup>38</sup>

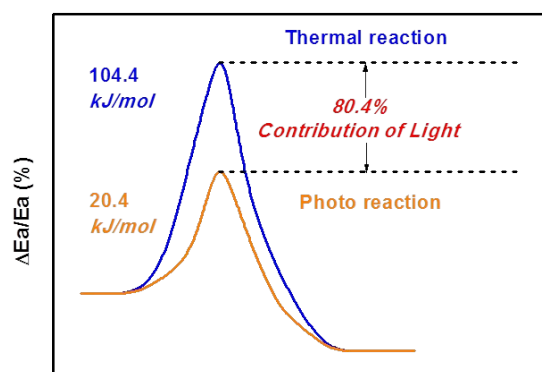


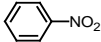
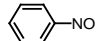
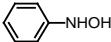
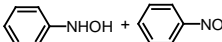
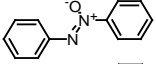
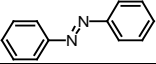
**Figure 8.** Apparent activation energies of nitrobenzene reduction calculated for the photoreaction and the reaction in the dark.

**Proposed mechanism**

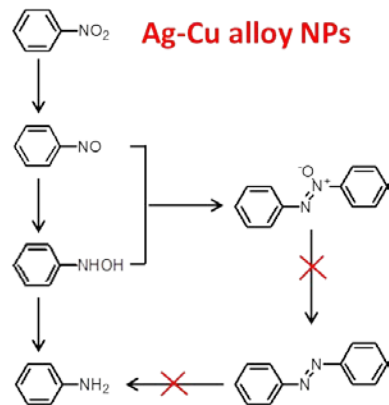
A widely accepted mechanism for the reduction of nitrobenzene was proposed by Haber in 1898 that nitro group stepwise reduced to aniline through nitroso- and hydroxylamine, additionally hydroxylamine is a highly active

intermediate causing the yield of azoxy and azo compounds,<sup>39</sup> the further reduction of azo compounds results in the hydroazo compounds which is eventually transformed into aniline.<sup>40-41</sup>

**Table 5.** Photocatalytic performance of Ag-Cu (4-1)@ZrO<sub>2</sub> using various intermediates as reactant.

Entry	Substrate	Conv. (%)	Select. (%)		
			Aniline	Azo	Azoxy
1		96	14	0	86
2 <sup>[a]</sup>		100	8	1	91
3 <sup>[a]</sup>		100	29	9	61
4 <sup>[a]</sup>		100	6	9	85
5		0	-	-	-
6		trace	-	-	-

Reaction condition: photocatalyst 50 mg, reactant 0.5 mmol, 3 mL IPA as solvent, 1 atm argon atmosphere, environment temperature 60°C, reaction time 16 h and the light intensity was 0.8 W/cm<sup>2</sup>. The conversions and selectivity were analysed by gas chromatography (GC). [a] reaction time 5 h.

**Scheme 1.** Possible reaction pathways for the reduction of nitrobenzene with Ag-Cu alloy NPs in the irradiation of visible light.

In this study, the fact that only azoxybenzene was obtained when using Ag-Cu Alloy NPs catalyst indicates a different reaction pathway regarding to the alloying of Cu and Ag (entry 1, Table 5.). First of all, the reduction of nitrobenzene over Ag-Cu alloy NPs produce azoxybenzene with minor aniline without other intermediates being detected. To further understand reaction route with Ag-Cu alloy NPs catalyst, several intermediates such as nitrosobenzene, hydroxylamine and azobenzene were used as substrates for the reduction to gain some insight into the reaction pathways.

In the Ag-Cu alloy NPs catalysed reaction system, trace aniline was obtained when using azoxybenzene and azobenzene as substrate (entries 5 and 6, Table 5.) indicating the azoxybenzene through azobenzene to aniline route is unfavorable. Therefore, it can be concluded the formation of aniline and azo-compound are parallel reactions. Compared with nitrobenzene, the reduction of nitrosobenzene and hydroxylamine is much faster. It is worth noticing that hydroxylamine gave greater yield to aniline than nitrobenzene and nitrosobenzene indicating its responsible to the direct production of aniline (entries 2 and 3, Table 5). When two intermediates were used together as the substrate, the similar selectivity to that of nitrobenzene was observed (entry 4, Table 5.). Hence, we proposed the reaction mechanism as shown in Scheme 1, Ag-Cu alloy NPs can catalyse the reduction of nitrobenzene through the coupling of nitrosobenzene and hydroxylamine, instead of further reducing to azobenzene or aniline. The Ag-Cu alloy NPs cannot transfer azoxybenzene into azobenzene possibly due to the limited reductive ability. Whereas monometallic Ag NPs could favour the further reduction of azoxybenzene to form azobenzene under the same conditions. (Table S2 and Scheme S1, ESI)

**Recycle of photocatalyst**

The reusability is a significant character of heterogeneous catalyst.<sup>42</sup> Therefore we performed the recycle experiment for the catalyst. The catalyst was reused for 10 times to test

the activity and the other reaction conditions were kept identical. After each reaction cycle, the catalyst was separated by centrifugation, washed with ethanol twice, and then dried for subsequent reactions. As shown in Figure 9, the catalyst was recycled for 10 times with less than 20% reduction of the catalytic activity. Noticeably, the selectivity to azoxybenzene can be still maintained above 70%. The observed slightly loss in catalytic activity was possibly due to the leaching of the NPs or the loss of NPs during washing after each catalytic run. To further confirm the heterogeneous nature of the alloy catalyst, we tested the amount of Ag and Cu in the reaction supernatant liquid by Inductively coupled plasma-atomic emission spectroscopic (ICP-AES) analysis, the amount of leaching was detectable (<10 ppm), but there was very little leaching of Ag during the reaction and the amount of the leached Cu decreased apparently with the recycle times (Table S4, ESI). We further conducted the hot filtration test,<sup>32</sup> as shown in Figure S3, the filtrate was incompetent to provide further conversion (only 8% increase), while the undisturbed control reaction showed excellent conversion (78% increase), which indicated that the filtrate solution did not contain a meaningful catalytically active species. Thus, overall it is evident that the reaction was predominately catalysed by the supported heterogeneous alloy NPs. The TEM image indicates that the Ag-Cu alloy NPs still distributed evenly after several times reactions, and the mean particle size remained 7 nm (Figure 10). These results confirmed that the Ag-Cu alloy NPs are stable and reusable photocatalyst for the reduction of nitrobenzene.

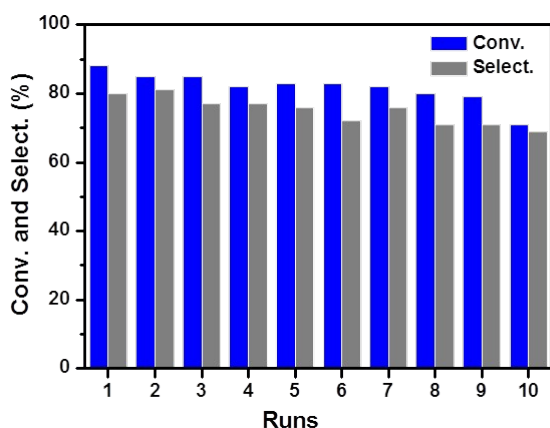


**Figure 9.** The reusability of the Ag-Cu alloy NPs for reduction of nitrobenzene under visible light irradiation. The selectivity is to azoxybenzene. Reaction conditions: photocatalyst 50 mg, reactant 0.5 mmol, 3 mL isopropyl alcohol (IPA) as solvent, 0.15 mmol KOH as base, 1 atm argon atmosphere, reaction temperature 60°C, reaction time 16 h and the light intensity was 0.8 W/cm<sup>2</sup>. The conversions and selectivity were analysed by gas chromatography (GC).

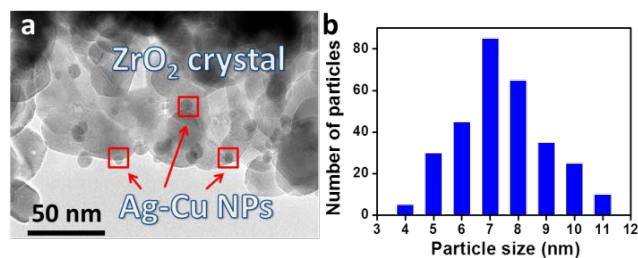


**Figure 10.** (a) TEM image of Ag-Cu (4-1)@ZrO<sub>2</sub> sample after 10 catalytic cycles. (b) Particle size distribution of Ag-Cu (4-1)@ZrO<sub>2</sub> sample after 10 catalytic cycles.

## Conclusion

In Summary, a green photocatalysis process for selective reduction of nitro compounds to azoxy compounds, driven by light irradiation without intensive heating and pressure reagent, can be achieved using Ag-Cu alloy NP catalyst prepared simply by alloying small amount of Cu into Ag NPs. The alloying of Cu into Ag NPs can maintain the azoxy compounds as main product, which is not easily controllable when using pure Ag NPs as catalyst. The catalyst with Ag-Cu ratio 4:1 exhibited the best photocatalytic performance and maintained stability in air. The selectivity to azoxybenzene and aniline can be controlled by turning the wavelength of irradiation. Meanwhile, the conversion of reactions can be enhanced with the rising of light irradiance and reaction temperature. The solid catalyst can be recycled and reused for several runs without significantly losing activity. The catalytic system provides us with a new direction for the application of alloy NP photocatalyst and also contribute to understanding the development of photocatalytic systems for more complex organic reactions driven by visible light under “green” mild conditions.

## Experimental section

### Catalysts preparation

3 wt% Ag-Cu alloy NPs on ZrO<sub>2</sub> (Ag-Cu alloy @ZrO<sub>2</sub>) with different ratios were prepared by the impregnation–reduction method. For example, Ag-Cu alloy NPs of molar ratio 4:1 was prepared as follow, AgNO<sub>3</sub> (82.3 mg) and Cu(NO<sub>3</sub>)<sub>2</sub>·6H<sub>2</sub>O (29.3 mg) was dissolved into 60 mL deionized water, to the above solution ZrO<sub>2</sub> nanopowder (2.0 g) was dispersed followed by adding 20 mL lysine aqueous (0.01 M) solution. The mixture was kept under magnetic stirring at room temperature for 20 min. To this suspension, 10 mL of freshly prepared aqueous NaBH<sub>4</sub> (0.35 M) solution was added dropwise. The mixture was aged for 24 h, and then the precipitate was separated by centrifugation, washed with water (three times) and ethanol (once), and dried at 60°C in vacuum for 24 h. The collected powder was used directly as catalyst. Other alloy catalysts with different Ag-Cu ratio, as well as NPs of pure Ag on the ZrO<sub>2</sub> support, were prepared via a similar method but using different amount of quantities.

### Catalysts characterisation

The morphology study of catalysts was carried out on a JEOL 2100 transmission electron microscopy (TEM) equipped with a Gatan Orius SC1000 CCD camera, with an accelerating voltage of 200 kV and nickel grids were used as the supporting film. Scanning electron microscope (SEM) imaging, elemental mapping and EDX were performed using a ZEISS Sigma SEM at accelerating voltages of 20 kV. Diffuse reflectance UV-visible spectra of the sample catalysts were examined by a Varian Cary 5000 spectrometer with BaSO<sub>4</sub> as a reference. X-ray photoelectron spectroscopy (XPS) data was acquired using a Kratos Axis ULTRA X-ray Photoelectron Spectrometer incorporating a 165 mm hemispherical electron energy analyser. The incident radiation was Monochromatic Al K $\alpha$  X-rays (1486.6 eV) at 225W (15 kV, 15 ma). Narrow high-resolution scans were run with 0.05 eV steps and 250 ms dwell time. Base pressure in the analysis chamber was 1.0x10<sup>-9</sup> torr and during sample analysis 1.0x10<sup>-8</sup> torr. X-ray diffraction (XRD) patterns of the sample powders were collected using a Philips PANalytical X'pert Pro diffractometer. Cu K $\alpha$  radiation ( $\lambda$ = 1.5418 Å) and a fixed power source (40 kV and 40 mA) were used. Inductively coupled plasma-atomic emission spectroscopic (ICP-AES) analysis was performed using a Perkin Elmer 8300DV ICP fitted with an ESI SC-4DX auto-sampler and PrepFAST 2 sample handling unit for online internal standardisation and auto-dilution of samples and calibration standards. Nitric acid, purified by sub-boiling distillation was used for the preparation of all standards and blank solutions used throughout the analysis.

### Activity test

In a typical activity test, a 20 mL Pyrex glass tube was used as the reaction vessel. The vessel containing reactants and catalyst was irradiated with visible light using a halogen lamp (from Nelson, wavelength in the range of 400–750 nm) under magnetic stirring; the irradiance was measured to be 0.8 W/cm<sup>2</sup>. The reaction temperature was carefully controlled with an air conditioner attached to the reaction chamber. The reactions in the dark were conducted using an oil bath placed above a magnetic stirrer to maintain the reaction temperature the same to corresponding reactions with light illuminations; reaction tubes were wrapped with aluminium foil to avoid exposure to light. At given irradiation time intervals, 0.5 mL aliquots were collected, the catalyst particulates was removed by a Millipore filter (pore size 0.45  $\mu$ m). The liquid-phase products were analysed by gas chromatography (GC) technique (Agilent 6890) with a HP-5 column to monitor the change in the concentrations of reactants and products. An Agilent HP5973 mass spectrometer was used to identify the product.

In action spectrum experiments, light emission diode (LED) lamps (Tongyifang, Shenzhen, China) with wavelengths 360 $\pm$ 5 nm, 400 $\pm$ 5 nm, 470 $\pm$ 5 nm, 530 $\pm$ 5 nm, 590 $\pm$ 5 nm and 620 $\pm$ 5 nm were used as light source. The reaction temperature was controlled with oil bath with all the other reaction conditions

identical to those of typical reaction procedures. The apparent quantum yield (AQY) was calculated as follow: apparent quantum yield = [(M<sub>light</sub> - M<sub>dark</sub>) / N<sub>p</sub>]  $\times$  100%, where M<sub>light</sub> and M<sub>dark</sub> are the molecules of products formed under irradiation and dark conditions respectively, M = mole number of the reactant  $\times$  conversion  $\times$  6.02  $\times$  10<sup>23</sup> (Avarado constant). N<sub>p</sub> is the number of photons involved in the reaction. N<sub>p</sub> = E<sub>total</sub> / E<sub>1</sub>, E<sub>total</sub> (the total energy involved in the reaction irradiation) = intensity  $\times$  light spot area  $\times$  reaction time, E<sub>1</sub> (the energy of one photon) = h  $\times$  c / L (h is Planck constant, c is light speed, L is wavelength of the LED light).

### Acknowledgements

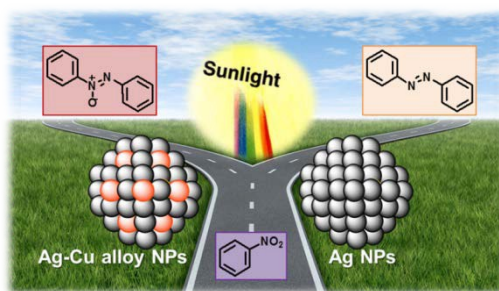
We gratefully acknowledge financial support from the Australian Research Council (ARC DP110104990 and DP150102110). We also thank Arixin Bo and Mitchell De Bruyn for the support of SEM and ICP analysis.

### Notes and references

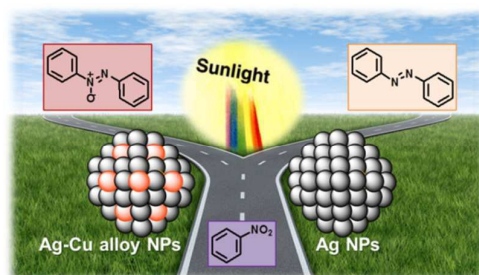
- 1 A. M. Tafesh and J. Weiguny, *Chem. Rev.*, 1996, **96**, 2035-2052.
- 2 L. He, L.-C. Wang, H. Sun, J. Ni, Y. Cao, H.-Y. He and K.-N. Fan, *Angew. Chem. Int. Ed.*, 2009, **48**, 9538-9541.
- 3 R. Mantha, K. E. Taylor, N. Biswas and J. K. Bewtra, *Environ. Sci. Tech.*, 2001, **35**, 3231-3236.
- 4 A.-J. Wang, H.-Y. Cheng, B. Liang, N.-Q. Ren, D. Cui, N. Lin, B. H. Kim and K. Rabaey, *Environ. Sci. Tech.*, 2011, **45**, 10186-10193.
- 5 F. Figueras and B. Coq, *J. Mol. Catal. A: Chem.*, 2001, **173**, 223-230.
- 6 J. M. Joseph, H. Destailats, H.-M. Hung and M. R. Hoffmann, *J. Phys. Chem. A*, 2000, **104**, 301-307.
- 7 S. S. Acharyya, S. Ghosh and R. Bal, *ACS Sustain. Chem. Eng.*, 2014, **2**, 584-589.
- 8 A. Agrawal and P. G. Tratnyek, *Environ. Sci. Tech.*, 1996, **30**, 153-160.
- 9 Y. Moglie, C. Vitale and G. Radivoy, *Tetrahedron Lett.*, 2008, **49**, 1828-1831.
- 10 K. Ohe, S. Uemura, N. Sugita, H. Masuda and T. Taga, *J. Org. Chem.*, 1989, **54**, 4169-4174.
- 11 A. Roucoux, J. Schulz and H. Patin, *Chem. Rev.*, 2002, **102**, 3757-3778.
- 12 A. Grirrane, A. Corma and H. García, *Science*, 2008, **322**, 1661-1664.
- 13 H. Zhu, X. Ke, X. Yang, S. Sarina and H. Liu, *Angew. Chem. Int. Ed.*, 2010, **49**, 9657-9661.
- 14 S. Sarina, H. Zhu, E. Jaatinen, Q. Xiao, H. Liu, J. Jia, C. Chen and J. Zhao, *J. Am. Chem. Soc.*, 2013, **135**, 5793-5801.
- 15 H. Zhu, X. Chen, Z. Zheng, X. Ke, E. Jaatinen, J. Zhao, C. Guo, T. Xie and D. Wang, *Chem. Commun.*, 2009, **48**, 7524-7526.
- 16 S. Linic, U. Aslam, C. Boerigter and M. Morabito, *Nat. Mater.*, 2015, **14**, 567-576.
- 17 J. C. Scaiano, K. G. Stamplecoskie and G. L. Hallett-Tapley, *Chem. Commun.*, 2012, **48**, 4798-4808.
- 18 H. Tada, T. Ishida, A. Takao and S. Ito, *Langmuir*, 2004, **20**, 7898-7900.
- 19 X. Chen, Z. Zheng, X. Ke, E. Jaatinen, T. Xie, D. Wang, C. Guo, J. Zhao and H. Zhu, *Green. Chem.*, 2010, **12**, 414-419.
- 20 X. Guo, C. Hao, G. Jin, H.-Y. Zhu and X.-Y. Guo, *Angew. Chem. Int. Ed.*, 2014, **53**, 1973-1977.
- 21 U. Sharma, P. Kumar, N. Kumar, V. Kumar and B. Singh, *Adv. Synth. Catal.*, 2010, **352**, 1834-1840.

- 22 A. Saha and B. Ranu, *J. Org. Chem.*, 2008, **73**, 6867-6870.
- 23 X. Liu, H.-Q. Li, S. Ye, Y.-M. Liu, H.-Y. He and Y. Cao, *Angew. Chem. Int. Ed.*, 2014, **53**, 7624-7628.
- 24 C. Morales-Guio, I. Yuranov and L. Kiwi-Minsker, *Top. Catal.*, 2014, **57**, 1526-1532.
- 25 L. Hu, X. Cao, L. Shi, F. Qi, Z. Guo, J. Lu and H. Gu, *Org. Lett.*, 2011, **13**, 5640-5643.
- 26 J. P. Espinós, J. Morales, A. Barranco, A. Caballero, J. P. Holgado and A. R. González-Elipe, *J. Phys. Chem. B*, 2002, **106**, 6921-6929.
- 27 M. Liu and W. Chen, *Nanoscale*, 2013, **5**, 12558-12564.
- 28 A. Marimuthu, J. Zhang and S. Linic, *Science*, 2013, **339**, 1590-1593.
- 29 G. Ranga Rao and H. R. Sahu, *J. Chem. Sci.*, 2001, **113**, 651-658.
- 30 A. Tanaka, S. Sakaguchi, K. Hashimoto and H. Kominami, *ACS Catal.*, 2013, **3**, 79-85.
- 31 E. Kowalska, R. Abe and B. Ohtani, *Chem. Commun.*, 2009, **2**, 241-243.
- 32 Q. Xiao, S. Sarina, E. Jaatinen, J. Jia, D. P. Arnold, H. Liu and H. Zhu, *Green. Chem.*, 2014, **16**, 4272-4285.
- 33 Q. Xiao, S. Sarina, A. Bo, J. Jia, H. Liu, D. P. Arnold, Y. Huang, H. Wu and H. Zhu, *ACS Catal.*, 2014, **4**, 1725-1734.
- 34 Q. Xiao, E. Jaatinen and H. Zhu, *Chem. Asian. J.*, 2014, **9**, 3046-3064.
- 35 Q. Xiao, Z. Liu, A. Bo, S. Zavahir, S. Sarina, S. Bottle, J. D. Riches and H. Zhu, *J. Am. Chem. Soc.*, 2015, **137**, 1956-1966.
- 36 S. Linic, P. Christopher and D. B. Ingram, *Nat. Mater.*, 2011, **10**, 911-921.
- 37 P. Christopher, H. Xin, A. Marimuthu and S. Linic, *Nat. Mater.*, 2012, **11**, 1044-1050.
- 38 S. Sarina, E. R. Waclawik and H. Zhu, *Green. Chem.*, 2013, **15**, 1814-1833.
- 39 K. Möbus, D. Wolf, H. Benischke, U. Dittmeier, K. Simon, U. Packruhn, R. Jantke, S. Weidlich, C. Weber and B. Chen, *Top. Catal.*, 2010, **53**, 1126-1131.
- 40 A. Corma, P. Concepción and P. Serna, *Angew. Chem. Int. Ed.*, 2007, **46**, 7266-7269.
- 41 H.-U. Blaser, *Science*, 2006, **313**, 312-313.
- 42 Y. Zhang, Q. Xiao, Y. Bao, Y. Zhang, S. Bottle, S. Sarina, B. Zhaorigetu and H. Zhu, *J. Phys. Chem. C*, 2014, **118**, 19062-19069.

## Table of contents



Photocatalytic reduction of nitroaromatics on Ag-Cu alloy NPs can maintain selectivity to azoxy compounds whereas Ag NPs mainly obtain azo compounds.

**Table of contents**

Photocatalytic reduction of nitroaromatics on Ag-Cu alloy NPs can maintain selectivity to azoxy compounds whereas Ag NPs mainly obtain azo compounds.

## Electronic Supplementary Information

**Selective reduction of nitroaromatics to azoxycompounds on supported Ag-Cu alloy nanoparticles through visible light irradiation**

Zhe Liu, Yiming Huang, Qi Xiao\* and Huaiyong Zhu

School of Chemistry, Physics and Mechanical Engineering, Science and Engineering Faculty, Queensland University of Technology, Brisbane, QLD 4001, Australia. E-mail: [q2.xiao@qut.edu.au](mailto:q2.xiao@qut.edu.au); Fax: +61 7 3138 1804; Tel: +61 7 3138 1581.

## LEGENDS

**Table S1.** The quantified composition of Ag and Cu for catalysts with different ratios

**Table S2.** Performance of Ag-Cu (4-1)@ZrO<sub>2</sub> for reduction of nitrobenzene with different substituent groups

**Table S3.** Photocatalytic performance of pure Ag@ZrO<sub>2</sub> using various intermediates as reactant

**Table S4.** The amount of Ag and Cu in the supernatant liquid after in the recycle of catalyst as detected by ICP-AES analysis

**Scheme S1.** Possible reaction pathways for the reduction of nitrobenzene with pure Ag NPs

**Figure S1.** Energy dispersive spectrometer (EDX) spectrum for Ag-Cu (1-1)@ZrO<sub>2</sub> and Ag-Cu (1-4)@ZrO<sub>2</sub> sample from TEM

**Figure S2.** Scanning electron microscopy (SEM) analysis of the catalysts

**Figure S3.** The results of the hot filtration test

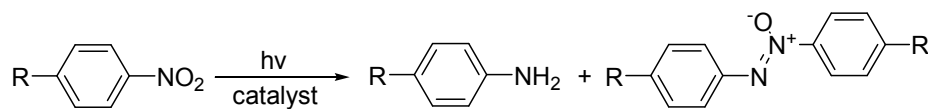
**Figure S4.** Transmission electron microscopy (TEM) analysis of the Ag NPs

**Table S1.** The quantified composition of Ag and Cu for catalysts with different ratios

Entry	Mole ratio of Ag to Cu		Weight ratio of Ag to Cu	
	Experimental design	TEM <sup>[a]</sup>	Experimental design	SEM <sup>[b]</sup>
1	4-1	4.3-1.0	2.6-0.4	2.65-0.35
2	1-1	1.4-1.0	1.9-1.1	1.97-1.03
3	1-4	1.0-4.4	0.9-2.1	1.05-1.95

[a] Determined from EDX spectrum and element mapping from TEM analysis in Figure 2e and Figure S2.

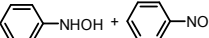
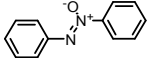
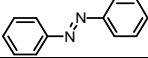
[b] Determined from EDX spectrum and elemental mapping from SEM analysis in Figure S3.

**Table S2.** Performance of Ag-Cu (4-1)@ZrO<sub>2</sub> for reduction of nitrobenzene with different substituent groups:

Entry	R	Conv. (%) (dark)	Select. (%)	
			Aniline	Azoxy
1	Cl	80 (46)	11	89
2	Br	70 (25)	29	71
3	MeO	50 (3)	29	71
4	H	96 (16)	14	86

Reaction condition: photocatalyst 50 mg, reactant 0.5 mmol, 3 mL isopropyl alcohol (IPA) as solvent, 0.15 mmol KOH as base, 1 atm argon atmosphere, reaction temperature 60°C, reaction time 16 h and the light intensity was 0.8 W/cm<sup>2</sup>. The conversions and selectivity were analysed by gas chromatography (GC).

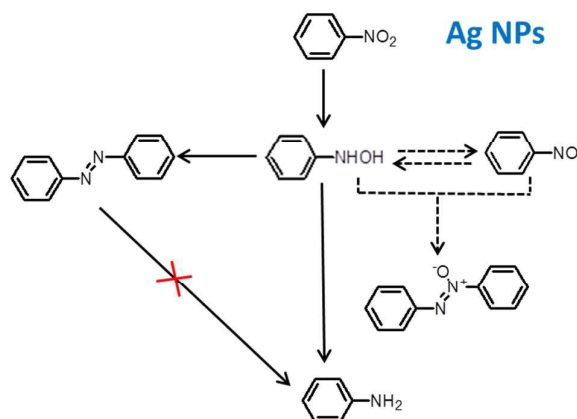
**Table S3.** Photocatalytic performance of pure Ag@ZrO<sub>2</sub> using various intermediates as reactant

Entry	Substrate	Conv. (%)	Select. (%)		
			Aniline	Azo	Azoxy
1		90	17	83	0
2 <sup>[a]</sup>		100	4	4	92
3 <sup>[a]</sup>		100	6	71	23
4 <sup>[a]</sup>		100	3	13	84
5		16	0	100	0
6		0	-	-	-

Reaction condition: photocatalyst 50 mg, reactant 0.5 mmol, 3 mL IPA as solvent, 1 atm argon atmosphere, environment temperature 60°C, reaction time 16 h and the light intensity was 0.8 W/cm<sup>2</sup>. The conversions and selectivity were analysed by gas chromatography (GC). [a] reaction time 5 h.

**Table S4.** The amount of Ag and Cu in the supernatant liquid after in the recycle of catalyst as detected by ICP-AES analysis

Entry	Runs	Amount of Ag (ppm)	Amount of Cu (ppm)
1	1	0.067	8.004
2	2	0.587	4.569
3	5	0.017	1.238
4	10	0.008	0.181

**Scheme S1.** Possible reaction pathways for the reduction of nitrobenzene with pure Ag NPs.

In the Ag NPs catalyst's case, we observed the same result as Ag-Cu NPs catalyst that azobenzene cannot be further reduce to aniline, it leads to same conclusion of formation of aniline and azocompound are parallel reactions (entry 6, Table S2). It was demonstrated Ag NPs cannot efficiently convert azoxybenzene into azobenzene (entry 5, Table S2), this phenomenon implies that in the reduction of nitrobenzene the great amount of azobenzene was not transferred from azoxybenzene but follows another pathway. On the other hand, when both nitrosobenzene and hydroxylamine was introduced into the reaction, we observed 84% yield of azoxybenzene (entry 4, Table S2). The reduction of nitrobenzene over Ag NPs catalyst cannot produce both nitrosobenzene and hydroxylamine otherwise azoxybenzene instead of azobenzene would have been observed. We separately investigated the reduction of nitrosobenzene and hydroxylamine and found reduction of hydroxylamine gives similar selectivity as the reduction of nitrobenzene only with faster reaction rate (entries 1 and 3, Table S2), however adverse selectivity was observed with nitrosobenzene (entry 2, Table S2). It illustrates the absence of nitrosobenzene as an intermediates in the reduction of nitrobenzene because if it exists stably in reaction system, azoxybenzene can be obtained as main product of coupling. Therefore, the complete reaction route of nitrobenzene reduction over Ag NPs catalyst is illuminated in Scheme S1.

Figure S1. The EDX spectrum from TEM

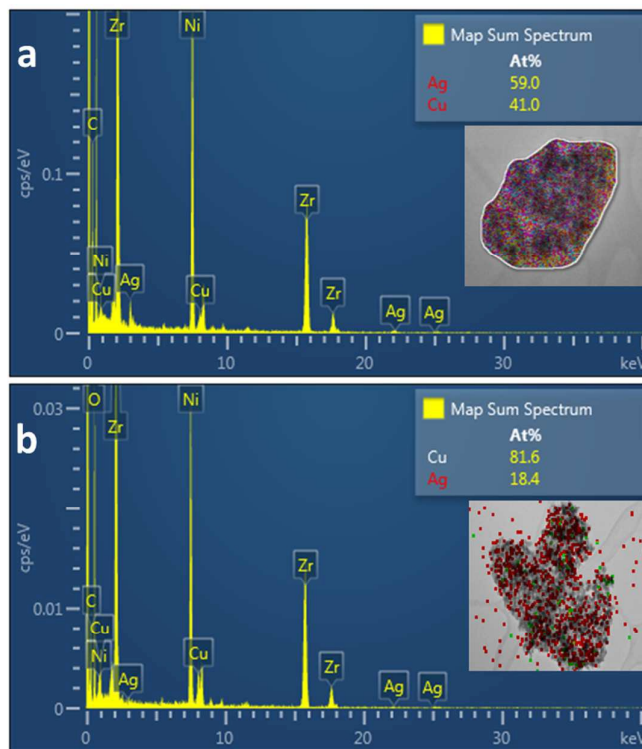
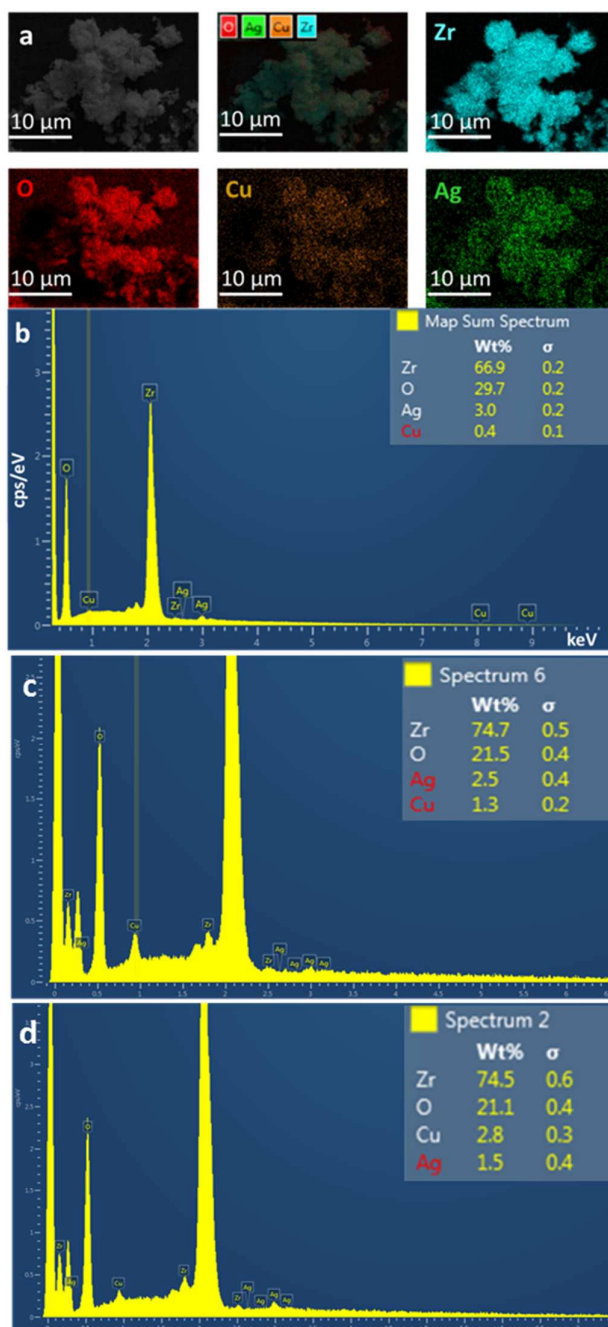
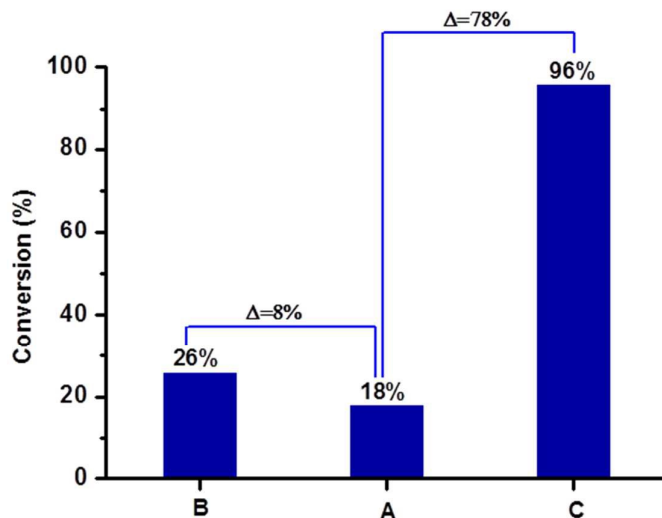
(a) EDX spectrum from TEM for Ag-Cu (1-1)@ZrO<sub>2</sub> samples. (b) EDX spectrum from TEM for Ag-Cu (1-4)@ZrO<sub>2</sub> samples

Figure S2. Scanning electron microscopy (SEM) analysis of the catalysts

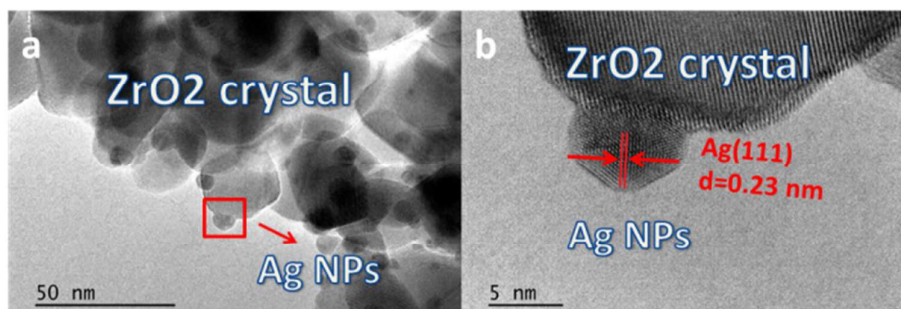


(a) SEM image of Ag-Cu (4-1) @ZrO<sub>2</sub> sample and the corresponding mapping of Zr, O, Cu and Ag elements. (b) EDX spectrum from SEM for Ag-Cu (4-1) @ZrO<sub>2</sub> sample. (c) EDX spectrum from SEM for Ag-Cu (1-1) @ZrO<sub>2</sub> sample. (d) EDX spectrum from SEM for Ag-Cu (4-1) @ZrO<sub>2</sub> sample.

**Figure S3.** The results of the hot filtration test

The reaction was interrupted at 1.0 h, and the catalyst was removed by filtration, the solution was labelled as A, 0.5 mL sample was collected for GC test. The rest solution without catalyst was re-irradiated as typical procedure, and after the reaction, sample was collected for GC test (labelled as B). After moving catalyst, the conversion for B increased by 8 % (from 18 % from 26 %). The conversion of typical reaction with catalyst (labelled C) was 96 %, which increased by 78 % from the first hour. It can be seen that the reaction did not proceed too much for the solution B, which means that the NPs peeled off from catalyst has little effect to the reaction. Moreover, from the reusability of Ag-Cu alloy NPs (Figure 9 in main text), we can also confirm that the catalytic activity doesn't lose too much during the reaction. Overall the main contribution of the activity results from the photocatalytic response of heterogeneous Ag-Cu alloy NPs.

**Figure S4.** Transmission electron microscopy (TEM) analysis of the Ag NPs



(a) TEM image of the Ag@ZrO<sub>2</sub> samples. (b) HR-TEM image of Ag particle indicated in part a (red square).